Hindawi
Advances in Civil Engineering
Volume 2022, Article ID 5642587, 10 pages
https://doi.org/10.1155/2022/5642587

Research Article

Research on the Anti-Leakage System for Reinforced Concrete Flat Roofs in Cold Areas

Li Lin,[1,2] **Xin Yuan**,[1] **Pengxiao Tang**,[1] **Xun Wang**,[1] **and Tianli Xu**[2]

[1]*College of Architecture Engineering, Harbin University of Science and Technology, Harbin 150080, China*
[2]*School of Civil Engineering, Harbin Institute of Technology, Harbin 150090, China*

Correspondence should be addressed to Li Lin; linli0119@163.com

Received 17 December 2021; Revised 15 April 2022; Accepted 23 April 2022; Published 6 May 2022

Academic Editor: Meisam Gordan

To solve the persistent problem of roof leakage in cold areas, a reinforced concrete flat roof anti-leakage prevention system was proposed in this study, and the leakage prevention of this roof system in the cold areas was investigated by conducting a scaled-down model outdoor exposure test. In addition, the weather in the Harbin area during the freeze-thaw cycle season was predicted by the support vector machine (SVM) model in machine learning, based on which ABAQUS finite element analysis of the roof system was carried out to reveal the leakage prevention mechanism of the system. The research results show that improving the roof level temperature during the freeze-thaw cycle can reduce the influence of temperature stresses brought by the freeze-thaw cycle, slow down the development of cracks inside the roof, reduce the probability of roof leakage, and can provide a new idea for solving the roof leakage problem in a cold area.

1. Introduction

China is a vast country with a wide distribution of cold regions, and water seepage in cold roofs has been a persistent problem [1]. To solve the problem of roof leakage, civil engineering workers, experts, and scholars have put forward many constructive ideas and solutions. In addition to conventional measures such as filling the roof with waterproofing materials and reconstructing the aging waterproofing layer, measures such as adding waterproofing layers to parts prone to leakage and using new materials with better waterproofing performance and greater durability are also widely used in roofing construction [2]. In the 1990s, Wu et al. [3] proposed the structural design of a pull-avoidance inverted waterproof roof. Bao et al. [4] adopted a pull-avoidance inverted roof structure and used gas barriers with a high vapor permeability resistance and thermal insulation materials with poor water absorption. Xu et al. [5] introduced new materials and technologies for roof construction in cold areas. Zhou et al. [6] discussed the causes of roof leakage in cold areas and provided several preventive measures. Lin and Li [7] put forward the practice of an anti-leakage drainage system for roofs in cold areas, which effectively reduced the influence of temperature stress on the roof system and improved the durability of roofs. Dong [8] proposed several construction options for separating the rigid surface layer from the asphalt waterproofing layer. Qu [9] found that the causes of cracking in the waterproofing layer can be attributed mainly to the deformation of the indirect joints in the prefabricated roof panels and the improper handling of the roof expansion joints. Zhao [10] proposed the installation of electric heating devices in roof drainage systems for buildings in cold regions.

Freeze-thaw cycles are one of the main causes of leakage in concrete roofs in cold areas. It can result in reduced performance of reinforced concrete, such as concrete strength decreases internal structural changes and tracking [11]. Since 1940, many scholars have studied the mechanism of freeze-thaw damage to the concrete from multiple angles and in all directions, conducting a large number of tests and drawing many valuable conclusions. Shang [12] performed bidirectional compressive stress tests on plain concrete specimens after 0, 25, 50, and 75 freeze-thaw cycles. Hasan [13], Penttala [14], and other scholars such as Sicat [15]

studied the stress-strain relationship in concrete during freeze-thaw cycles. The destruction mechanism of concrete under repeated freeze-thaw cycle was summarized; typical research could be found in Zhang et al. [16] Tian and Zhang [17], Chen and Cui [18], and Liang et al. [19].

To sum up, existing research has mainly focused on adding a waterproofing layer to the parts prone to leakage or using new materials with better waterproofing properties; however, this method ignores the impact of freeze-thaw cycles on the roof leakage in cold regions and can only solve surface problems, making it difficult to completely eradicate the leakage phenomenon.

In this study, the anti-leakage system of reinforced concrete flat roofs in cold areas is proposed, which is different from the traditional leakage prevention structure, and it can resist the freeze-thaw cycle by raising the roof temperature, improving the durability of concrete, and solving the problem of roof leakage. In addition to outdoor exposure tested on the scaled-down model of reinforced concrete roof leakage prevention system in cold regions, the freeze-thaw cycle occurrence time and temperature were predicted by the support vector machine (SVM) [20–22], and ABAQUS finite element simulations were performed on the roof system based on the prediction results to study the roof leakage prevention performance.

2. Design of an Anti-Leakage System for Reinforced Concrete Flat Roofs

In actual engineering, a roof panel without measures against freeze-thaw cycles will produce cracks that continue to grow, causing a large-area leakage. The key to solving the problem of roof leakage in cold areas is to reduce the stress generated by the roof panels during the freeze-thaw cycle. Therefore, this study proposes an anti-leakage system for reinforced concrete flat roofs constructed in cold areas. The system comprises three parts: the main body of the roof system, a heating system, and a drainage system, as shown in Figure 1.

The design idea is to add a heating system to the main body of the roof system, utilize the heat radiation effect of the heating system to increase the overall temperature of the roof, prevent the roof from freezing, reduce the stress generated by the roof in the freeze-thaw cycle, and establish a drainage system to facilitate the rapid discharge of the roof snow after melting; the three parts of the system together can help resist freeze-thaw cycles. The main body of the roof system comprises a load-bearing roof slab, a pre-buried pipeline insulation layer, a slope layer, a leveling layer, a waterproof layer, and a protective layer, as shown in Figure 2. The main body of the roof system uses multiple water dividers to make the longitudinal section of the roof in the shape of a folded plate while maintaining a drainage slope ranging from 2% to 5%, and water outlets are evenly arranged between adjacent roof ridges to facilitate the rapid collection of water on the roof, thus completing the optimization of the drainage of the roof panels. The roof heating system comprises a circulating water supply system, a heating branch pipe pre-buried in the roof, a water supply main pipe, a water return main pipe, and a water stop valve. The roof drainage system is arranged horizontally

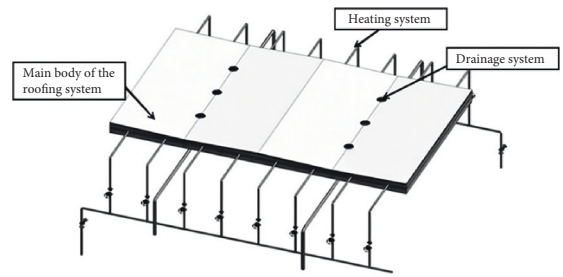

Figure 1: Overall diagram of the anti-leakage system of reinforced concrete flat roofs constructed in cold regions.

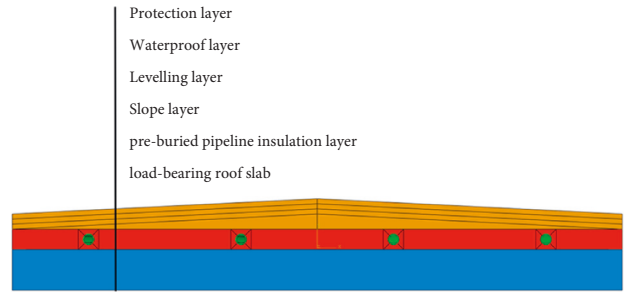

Figure 2: Schematic of the main roof system.

along the building using suspension pipes parallel to the ridgeline, and the suspension pipe branches are connected to the roof drop inlets.

When a freeze-thaw cycle occurs, the heating system is switched on, so that the thermal medium in the roof insulation layer carries out thermal radiation to raise the overall temperature of the roof system. The snow on the roof is heated and melted, and it flows into the roof dropout to be discharged through the drainage pipe to reduce the accumulation of water on the roof and prevent roof cracks when the solid-liquid conversion of water aggravates the roof. Thus, the problem of roof leakage in cold areas is solved.

3. Outdoor Exposure Test for Reinforced Concrete Flat Roof Scaled-Down Models

The most direct way to verify the ability of an anti-leakage system for reinforced concrete flat roofs to resist freeze-thaw cycles is to place the roof system in a freeze-thaw cycle environment and observe its insulation capacity and temperature field distribution in a natural low-temperature environment. By collecting the temperature information of the roof under the natural environment exposure, the performance of the roof system to resist freeze-thaw cycles in the natural environment is analyzed. The test is based on the provision of the national standard specification "Standard for testing methods of long-term performance and durability of ordinary concrete" (GB/T50082-2009) [23], concerning the slow freezing method test method.

3.1. Test Program. A scaled-down model of the reinforced concrete flat roof system was made and connected to the heating system. Four measurement points were arranged at

different locations on the scaled-down model from the heating pipes to measure the temperature changes. An ambient temperature group was added as a control group to study the influence of the heating system on the overall temperature of the roof system and to verify the insulation capacity of the roof system and its resistance to freeze-thaw cycles. Figure 3 shows the measurement point layout.

The scaled-down model was placed in an outdoor environment, and the test was started by energizing the CNC pump and electric heating rod to work the heating system. The test time was 12 h, and the test data were recorded using a THTE multiplex PID temperature controller.

3.2. Model Production and Test Preparation. The main materials used to prepare a scaled-down model of a reinforced concrete flat roof impermeability system were C30 concrete, 1 : 8 cement perlite material, 1 : 2.5 ordinary silicate cement mortar, 3 mm thick SBS-modified bitumen waterproofing membrane waterproofing layer, and cast iron pipes with an internal diameter of 19 mm and an external diameter of 22 mm. Among them, the size of the coarse concrete aggregate was in the range of 5–40 mm, and the cement, river sand, and coarse aggregate required in the preparation process were collected from Heilongjiang Province. The mixing water used was tap water.

After completing the material preparation for modeling, the structural floor slab formwork was first erected to ensure that the structural floor slab size was 1200 mm × 400 mm×80 mm. After the formwork was fixed, C30 concrete was poured and vibrated, and water was poured after 12 h for maintenance. After 14 days of maintenance, the formwork for the predetermined cast iron pipe holes was erected on the concrete slab, the cast iron pipe with an internal diameter of 19 mm and an external diameter of 22 mm was buried in the designed position, and the concrete was poured again to complete the construction of the insulation layer. Thereafter, a slope of 3% was laid on the insulation layer, 1 : 8 cement perlite material was laid from both sides of the roof towards the center, the slab was vibrated and paved, and the surface was scraped with a scraping bar and smoothed with a trowel. The slope layer on the paving material was 1 : 2.5 ordinary silicate cement mortar leveling layer, paving after maintenance for seven days. Finally, a 3mm thick self-adhesive SBS modified bitumen waterproofing roll-roofing membrane was laid, and and water storage test was carried out on the waterproof layer 24h after completion of laying, to confirm that there was no leakage on the roof, and then the protective layer was poured and maintained; the complete production of reinforced concrete flat roof antileakage system scaled-down model is shown in Figure 4.

Finally, the scaled model was connected to a water tank, CNC water pump, and water supply pipe; in turn, electric heating rods were placed in the water tank, Pt100 type RTDs were glued at the measurement points of the scaled model, and resistors were connected to the THTE multi-way PID temperature controller for temperature data recording. This completed the connection between the scaled model and the heating system and the arrangement of the data acquisition device. Figure 5 shows the overall layout of the outdoor exposure test of the scaled-down model of the reinforced concrete flat roof leakage prevention system.

3.3. Test Results. At the end of the test, the data recorded by the temperature controller were exported, and the time-temperature curve for each measurement point was obtained by processing the test data, as shown in Figure 6. The overall temperature increase in the roof system was significant; with the change in the ambient temperature, the overall temperature at the four measurement points increased to different degrees, but the overall temperature at the four measurement points of the roof still had a significant difference. The temperature was highest at measurement point 1, followed by measurement point 4, measurement point 3, and lastly measurement point 2. The temperature curves at the four measurement points also had different fluctuations. The curve for measurement point 1 was the smoothest, and fluctuations were the lowest; the fluctuations in the curve for measurement point 2 were the highest, and the fluctuations in the curves for measurement points 3 and 4 were in between. Furthermore, the initial temperature at measurement point 1 was −16°C, slightly above the initial ambient temperature of −18°C, while the other three measurement points were at the same temperature as the ambient temperature. The reason for the different temperature variations at each measurement point is that point 1 was located in the insulation layer, closest to the heating line. Therefore, it had a higher initial temperature than the ambient temperature and the highest overall temperature and was less susceptible to changes in the ambient temperature, with the lowest fluctuations in the temperature profile. Point 2 was located at the corner of the roof, the furthest from the heating line; it exhibited the lowest overall temperature, was most influenced by the ambient temperature, and had the most fluctuating curve. Point 3 was located on the ridge and had a lower overall temperature, but due to the heating lines on both sides, point 3 was less affected by the ambient temperature than point 2 and had a higher overall temperature than point 2. Point 4 was not in the insulation layer, but the distance from the heating pipeline was second only to point 1; therefore, the overall temperature was less than that at point 1 and higher than those at points 2 and 3.

Under the continuous application of the temperature field by the heating system, the overall temperature of the roof system increased more evidently, which effectively reduced the temperature stress due to the fluctuation of the roof system in practice and decreased the probability of leakage of the roof system under the freeze-thaw cycle. This proves the effectiveness of the proposed leakage prevention system for reinforced concrete flat roofs in cold areas.

4. Numerical Analysis

The numerical analysis of freeze-thaw cycles of reinforced concrete flat roof systems in cold regions requires the collection of corresponding weather data, which are entered

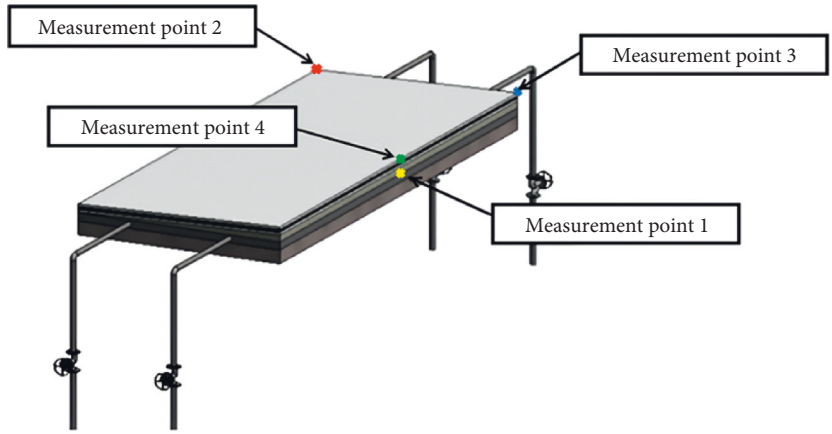

Figure 3: Temperature measurement point layout.

Figure 4: Scaled-down model of the anti-leakage system for reinforced concrete flat roofs.

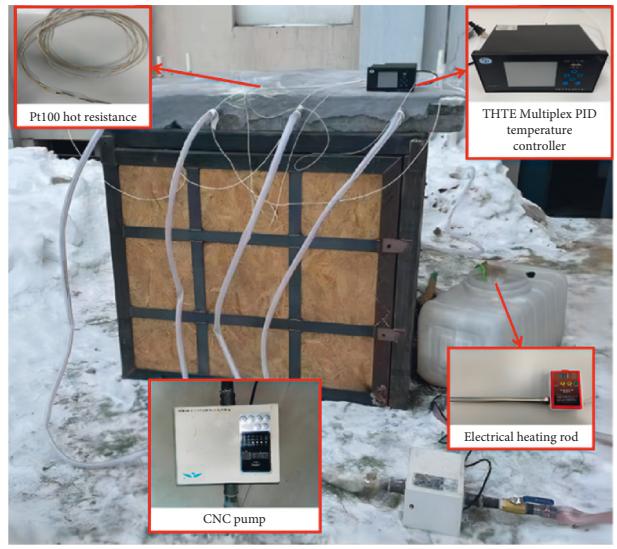

Figure 5: Overall layout of an outdoor exposure test.

into the numerical analysis model as a temperature boundary condition; however, the outdoor collection has disadvantages such as long lead time and instability. Therefore, based on the weather information of Harbin during the freeze-thaw cycle-prone seasons of March and November, this study combines the SVM model of machine learning [24].

4.1. SVM Algorithm Prediction Model. SVM models have supervised learning models associated with relevant learning algorithms and are mainly used to analyze data, identify patterns, and perform classification and regression analysis studies. SVM maps the sample space to a high or even infinite-dimensional feature space through nonlinear mapping, in which a linear learning machine approach is applied to solve problems such as the highly nonlinear classification and regression in the sample space. In the SVM model, the generalized error is determined by three parameters, namely the cost parameter (E), the tolerance parameter (ε), and the kernel parameter (γ), and the values of these three parameters are not unique. Referring to Cherkassky and Ma [25], the SVM model parameters are determined according to equations (1)–(5); Table 1 presents the model parameters. The correlation coefficient R indicates the degree of correlation between the estimated and true values, and the higher the correlation coefficient R, the better the correlation.

$$E = \max\left(\left|\overline{y} + 3\sigma_y\right|, \left|\overline{y} - 3\sigma_y\right|\right), \tag{1}$$

where $\overline{y}$ and σ_y are the mean and standard deviation of the training data Y values, respectively, expressed as follows:

$$\gamma = \frac{1}{2\rho^2}, \tag{2}$$

$$\rho = m\sqrt[k]{0.3}, \tag{3}$$

$$\varepsilon = 3\sigma\sqrt{\frac{\ln n}{n}}, \tag{4}$$

$$\delta = y_i - f(x_i), \tag{5}$$

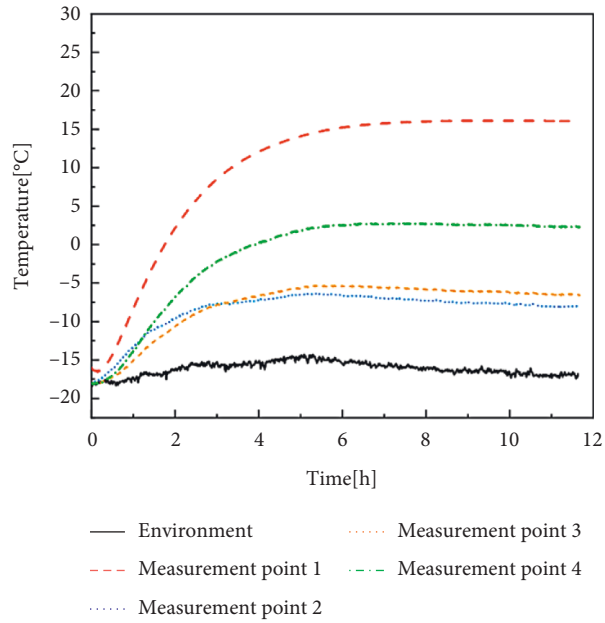

Figure 6: Time-temperature curves of each measurement point in the outdoor exposure test.

Table 1: Parameters of the SVM model.

Object	E	ε	γ	Mean absolute error	Mean squared error	R
Minimum air temperature	5.4796	0.1499	0.1174	0.5754	0.5133	0.7786
Maximum air temperature	6.7112	0.1378	0.1184	0.4478	0.4208	0.8432

where k is the number of output variables, m is the range of input values, σ is the difference between the true and predicted values, n is the number of values y, and δ is the standard deviation of the residuals.

Figure 7 shows the predicted maximum and minimum temperatures for the freeze-thaw cycle season in the Harbin area, where the serial number represents the weather number for the freeze-thaw cycle season, and the maximum and minimum temperatures represent the predicted values for the maximum and minimum temperatures for the day. The square set of dots in the graph is the simulated maximum temperature of the day in Harbin. The magnitude of the value increases with the serial number and then decreases, and the rate of increase is small at first, gradually increases with the serial number, increases rapidly after the serial number reaches 10, reaching the highest value at serial number 37, and then gradually decreases. The set of circles in the graph is the predicted minimum temperature for the day. The trend in the minimum temperature for the day is similar to that for the maximum temperature, both increasing and then decreasing. At the same time, between serial numbers 16–24 and 38–56, the highest temperature of the day is greater than 0°C, and the lowest temperature of the day is less than 0°C; therefore, the time interval in which the freeze-thaw cycling effect should occur must be between the two intervals of serial numbers 16–24 and 38–56. The temperature data within this time interval are extracted to obtain the SVM prediction of the temperature amplitude in which the freeze-thaw cycling effect may occur, as shown in Figure 8.

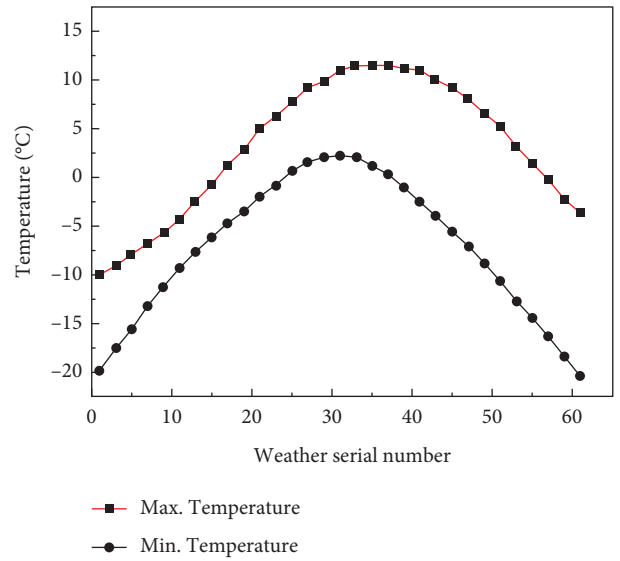

Figure 7: SVM predicts the daily maximum and minimum temperatures.

4.2. Establishment of the Numerical Analysis Model. The finite element analysis software ABAQUS was used to establish a numerical analysis model of the flat roof leakage prevention system for reinforced concrete in cold zones. The finite element model components include a structural floor slab, an insulation layer, pre-buried pipelines, and an upper maintenance structure, assembling each component to form

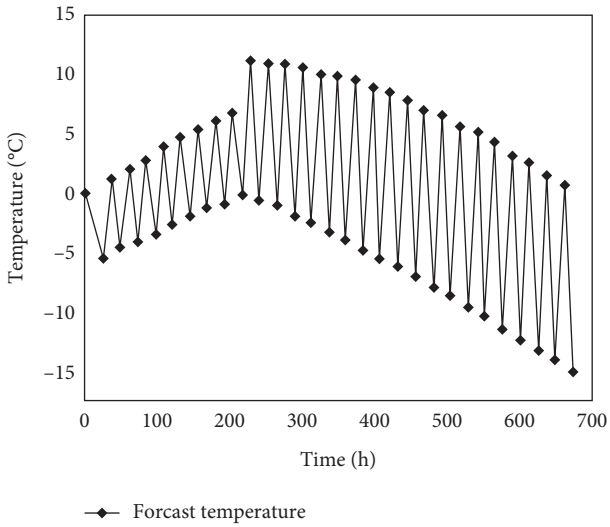

Figure 8: SVM predicts the temperature amplitude at which freeze-thaw cycles may occur.

a complete roof body model. Figure 9 shows the analytical model.

The numerical simulation was divided into two parts: a heat transfer analysis and static analysis. A given temperature amplitude was inputted into the analysis model for the heat transfer analysis, and the temperature field obtained from the heat transfer analysis was then imported into the experience analysis as a prestress field, resulting in the temperature stress distribution. The C3D8R and C3D20R units were used for the heat transfer and static analyses of the main roof components, respectively. The concrete material parameters were defined in terms of the density, thermal conductivity, and specific heat capacity for the heat transfer analysis and in terms of the modulus of elasticity, coefficient of linear expansion, and concrete damage for the static analysis. During the static analysis, only three parameters, namely the density, thermal conductivity, and specific heat capacity, were defined for the upper maintenance structure materials, namely the cement perlite, cement mortar, waterproof membrane, and cast iron, as the stress changes in the upper envelope had a small impact on the crack development condition of the roof body. Tables 2 and 3 present the model material parameters. In the actual project, the roof body parts work together. Therefore, the model components are bound to each other and considered as a whole. A hinge restraint is applied to the bottom of the roof body to ensure that the bottom slab of the roof body is not displaced.

4.3. Numerical Analysis in the SVM Prediction. Four test points were arranged in the model, corresponding to the outdoor exposure test points of the scaled model, as shown in Figure 10.

The SVM-predicted temperature amplitude of the possible freeze-thaw cycles as a boundary condition was inputted into the model for the heat transfer analysis, and the temperature change curves at each measurement point under the SVM-predicted environment were obtained, as shown in Figure 11. The temperature at all the measurement points on the roof under the freeze-thaw cycle first increases and then decreases, while the temperature change law at each measurement point is consistent with the temperature change law at each measurement point in the outdoor exposure test. The overall temperature at measurement point 1 is the highest, and the temperature fluctuation is the smallest; the overall temperature at measurement point 2 is the lowest, and the temperature fluctuation is the highest; the temperature at measurement points 3 and 4 is between those at measurement points 1 and 2; however, the overall temperature at measurement point 4 is higher than that at the measurement point 3. In addition, the temperatures at all the four measurement points were above 0°C by 576 h. Among these, all the parts of the temperature, including the temperature of the low-temperature zone, which is widely distributed on the roof, were always above 0°C, except at measurement point 2, which is at the edge of the roof system, where the temperature decreased below 0°C. This proves the insulation capacity of the reinforced concrete flat roof leakage prevention system in cold regions in a freeze-thaw cycle environment.

The temperature field obtained from the heat transfer analysis was introduced into the static analysis step as a prestress field. Three measurement points were arranged, and the temperature stress distribution of the roof system was analyzed to obtain a temperature stress cloud for the main body of the roof, as shown in Figure 12. There is significant temperature stress in the main body of the roof concrete under the effect of freeze-thaw cycles. The deformation of the main body of the roof is influenced by the hinge restraint at the bottom surface, which is in the shape of a narrow prism at the bottom and a wide prism at the top, with a significant stress concentration at the bottom corners, reaching a maximum of approximately 24.54 MPa. The temperature stress distribution in the main concrete of the roof is generally decreasing from bottom to top, and there is a certain stress concentration in the pre-buried heating pipes.

The stress variation curves at the three measurement points of the roof are extracted and shown in Figure 13. After experiencing sequential temperature stress coupling, the temperature stresses at measurement points 2 and 3 tend to fluctuate, with the maximum values reaching 6.53 and 4.85 MPa, respectively. The stress at measurement point 1 tends to rise and then level off, with a small variation and a maximum value of approximately 0.53 MPa. Due to the large temperature variations at measurement points 2 and 3, greater temperature stress is generated in the static analysis relative to that at measurement point 1, while measurement point 1 has a smaller temperature variation, and its temperature stress grows more gradually during the freeze-thaw cycle. After a predicted freeze-thaw cycle, the overall temperature stress on the roof system is low, and the concrete in the roof system is in the elastic strain phase except for the hinged position. The reinforced concrete flat roof leakage prevention system in the cold zone can control the temperature stress at a low level and improve the leakage resistance of the concrete.

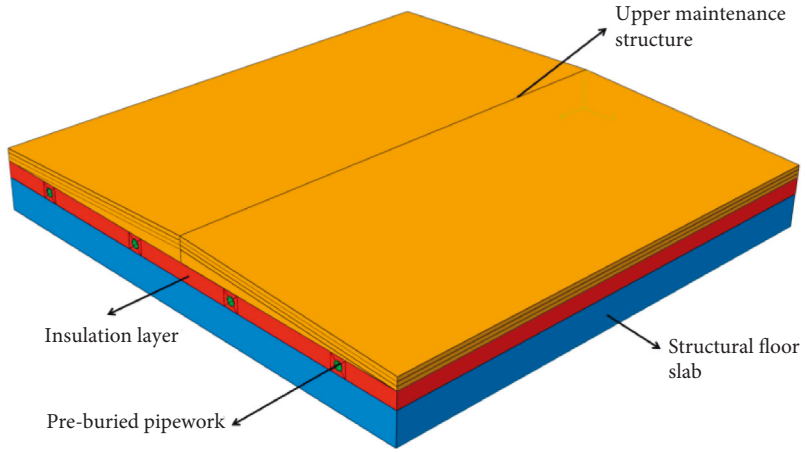

Figure 9: Analysis model.

Table 2: Material thermodynamic parameters.

Material	Thermal conductivity/(W/(m·K))	Specific heat capacity/(J/(kg°C))	Density/(kg/m^3)	Modulus of elasticity/(MPa)	Linear expansion coefficient/(m/°C)
C30 concrete	1.74	0.92	2500	30000	8×10^{-6}
Cement pearl rock	0.21	1.17	600	—	—
Cement mortar	0.93	1.05	1800	—	—
Waterproofing roll roofing	0.17	1.47	600	—	—
Iron casting	49.9	0.48	7250	—	—

Table 3: Concrete plastic damage parameter.

Material	Expansion angle	Poisson's ratio	Coefficient of viscosity	Eccentricity	K	f_{c0}/f_{b0}
C30 concrete	30	0.2	0.005	0.1	0.667	1.16

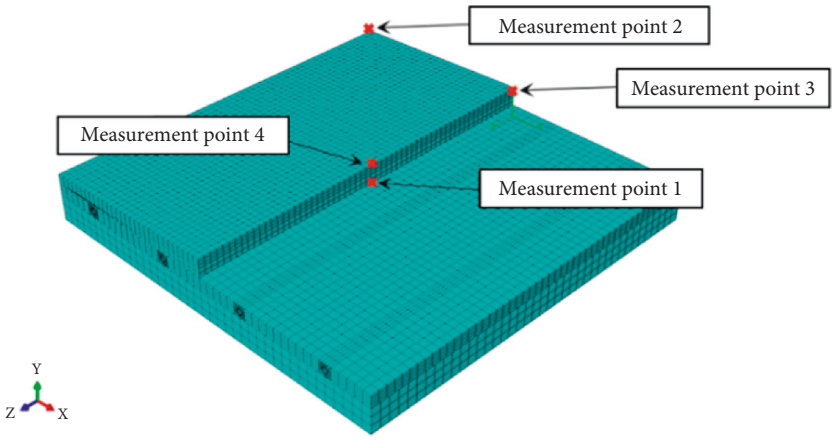

Figure 10: Layout of temperature measuring points in the numerical model.

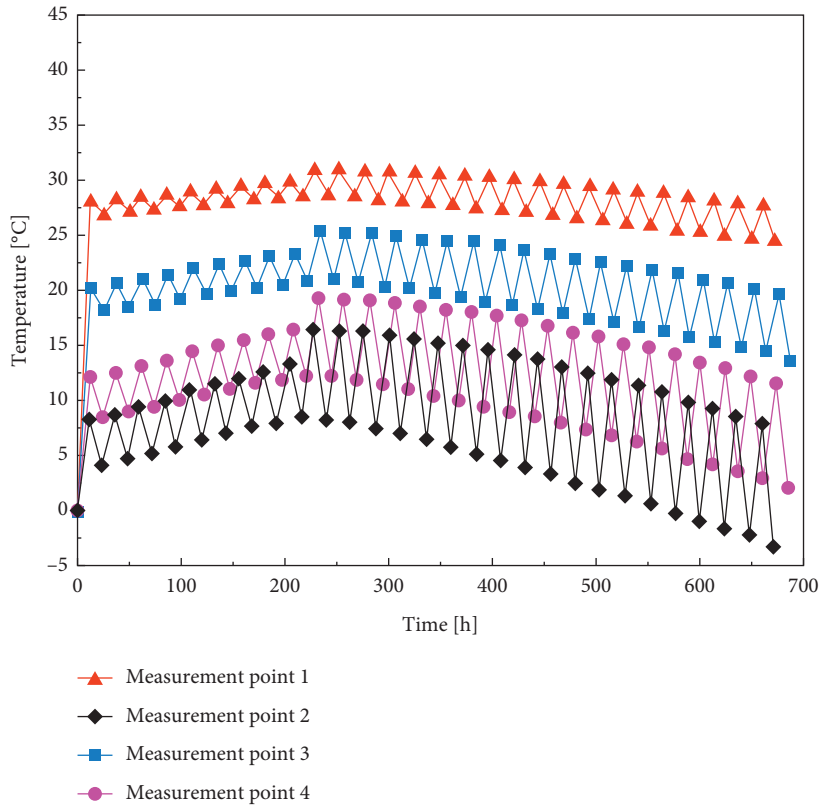

Figure 11: SVM predicts the temperature at each measuring point in the SVM-predicted environment.

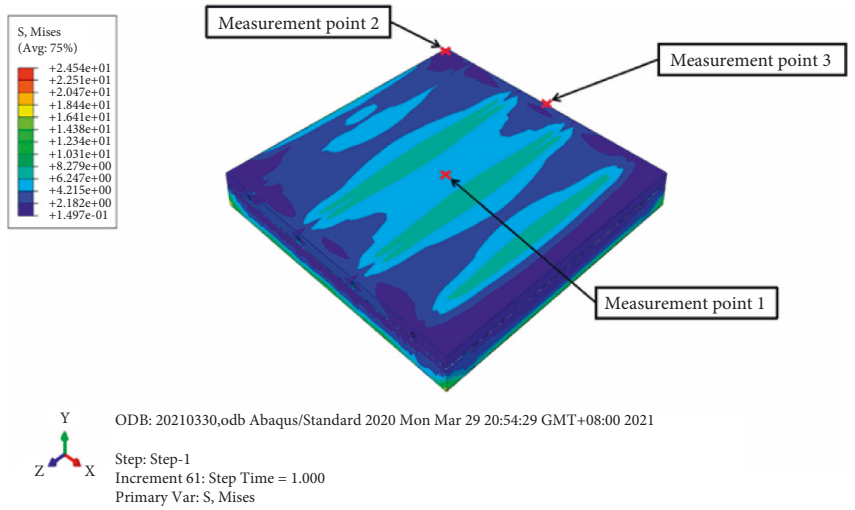

Figure 12: Temperature stress cloud.

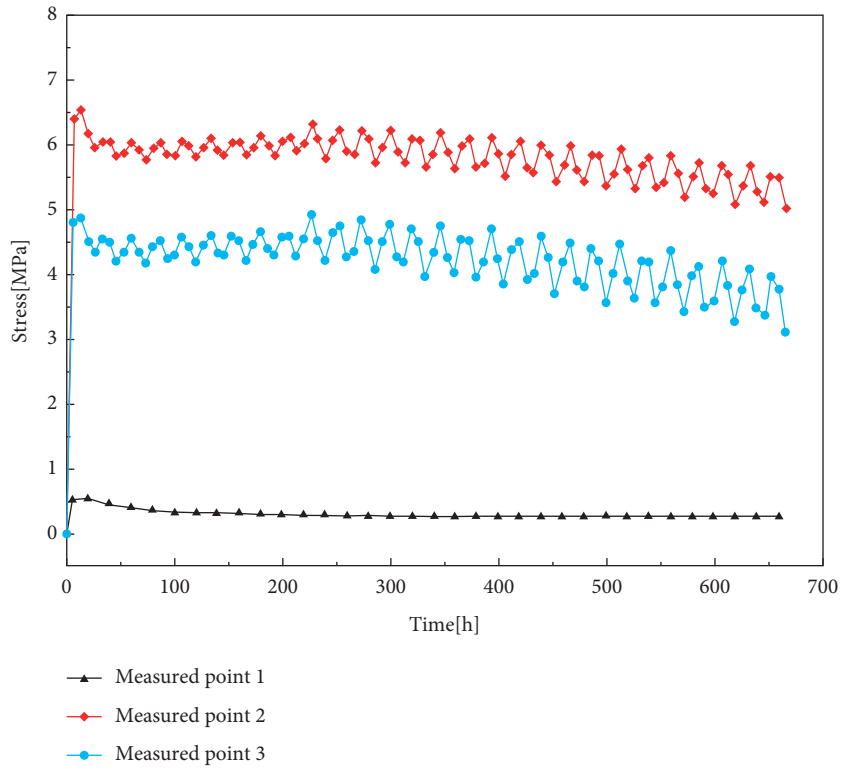

Figure 13: Time-temperature stress curve.

5. Conclusions

This study developed an anti-leakage system for reinforced concrete flat roofs constructed in cold regions and prepared a scaled-down model for outdoor exposure tests to verify the resistance of the system to freeze-thaw cycles. A weather prediction model based on the machine learning SVM algorithm was established, and a numerical analysis model of the freeze-thaw cycle of a flat roof leakage prevention system for reinforced concrete in cold zones was built on this basis. The response of the proposed leakage prevention system under the effect of the freeze-thaw cycle was numerically analyzed to reveal the leakage prevention mechanism of the system. The main results and conclusions are as follows:

(1) The working principle of leakage prevention system for reinforced concrete flat roofs in cold areas is to add a heating system to the main roof system, utilize the heat radiation effect of the heating system to increase the overall temperature of the roof, prevent the freezing of rainwater on the roof, and reduce the stress generated by the freeze-thaw cycle. The drainage system is also installed to facilitate the rapid discharge of snow water after melting.

(2) The roof system has good thermal insulation performance after adding the heating system; the temperature at all locations on the roof increased under the continuous application of the temperature field of the heating system, effectively resisting the freeze-thaw cycle, proving that the system designed has good resistance to freeze-thaw cycles.

(3) The SVM model predicted that freeze-thaw cycles are likely to occur on 26 days during the freeze-thaw cycle-prone season in Harbin, and the maximum temperature amplitude of the freeze-thaw cycle during this period is 18°C.

(4) The ABAQUS finite element simulation of the roof system based on the prediction of the SVM model found that the roof heating system could effectively reduce the effect of temperature stress caused by the freeze-thaw cycle, delay the development of internal cracks in the roof, and reduce the occurrence of roof leakage. It verified the impermeability of the roof system under the effect of the freeze-thaw cycle.

Data Availability

The data used to support the findings of this study are included within the article.

Conflicts of Interest

The authors declare that they have no conflicts of interest.

Acknowledgments

The authors wish to acknowledge the support provided by the National Science Foundation of Heilongjiang Province of China (no. LH2019E060) and the National Nature Science.

References

[1] Z. Wen, "Analysis of the causes of building roof leakage and research on anti-seepage disposal measures," *Green Environmental Protection Building Materials*, vol. 11, pp. 141-142, 2020, in Chinese.

[2] J. Gui, J. Gu, and X. Zhou, "Roof anti-seepage control technique of new waterproof and heat insulation material," *Architectural Technology*, vol. 46, no. 07, pp. 629–632, 2015, in Chinese.

[3] P. Wu and G. Zhang, "Pull-avoidance inverted roof is used in cold areas," *Low Temperature Architecture Technology"*, vol. 3, pp. 24-25, 1995, in Chinese.

[4] P. Bao and X. Bai, "Problems and countermeasures in the existing roofing structure in cold areas," *Anhui Architecture*, vol. 3, pp. 55-56, 1998, in Chinese.

[5] A. Xu and Y. Chen, "Application of thermal insulation and energy saving technology for building roof in cold area," *Heilongjiang Hydraulic Science and Technology*, vol. 1, pp. 118-119, 2004, in Chinese.

[6] Q. Zhou, "Discussion on the causes and control measures of roof leakage in cold areas," *Heilongjiang Science and Technology Information*, vol. 4204 pages, 2007, in Chinese.

[7] J. Li, *Some Problems about Transfer Story Buildings in Cold Regions Based on BIM*, Harbin University of Science and Technology, Harbin, China, 2018, in Chinese.

[8] C. Dong and S. Cui, "Exploring the design of upstander roofing structures in cold areas," *Architectural Technology*, vol. 10, pp. 611-612, 1993, in Chinese.

[9] F. Qu, B. Zhang, and S. Xu, "Exploration of crack leakage in roof waterproofing projects in cold areas," *Low Temperature Architecture Technology*, vol. 041999, in Chinese.

[10] S. Zhao and W. Wang, "Research on frost protection technology for large roof drainage systems in cold regions," *Construction Science and Technology*, vol. 23, pp. 94-95, 2014, in Chinese.

[11] R. Guo and H. Shang, "Bond behaviour of reinforced recycled concrete after rapid freezing thawing cycles," *Cold Regions Science and Technology*, vol. 157, pp. 133–138, 2018.

[12] H. S. Shang and Y. P. Song, "Experimental study of strength and deformation of plain concrete under biaxial compression after freezing and thawing cycles," *Cement and Concrete Research*, vol. 36, no. 10, pp. 1857–1864, 2006.

[13] M. Hasan, T. Ueda, and Y. Sato, "Stress-strain relationship of frost-damaged concrete subjected to fatigue loading," *Journal of Materials in Civil Engineering*, vol. 20, no. 1, pp. 37–45, 2008.

[14] V. Penttala and F. A. Neshawy, "Stress and strain state of concrete during freezing and thawing cycles," *Cement and Concrete Research*, vol. 32, no. 9, pp. 1407–1420, 2002.

[15] E. Sicat, F. Gong, T. Ueda, and D. Zhang, "Experimental investigation of the deformational behavior of the interfacial transition zone (ITZ) in concrete during freezing and thawing cycles," *Construction and Building Materials*, vol. 65, pp. 122–131, 2014.

[16] S. Zhang, M. Deng, and M. Tang, "Research progress of freeze and thaw cycle destruction of concrete," *Journal of Materials Science and Engineering*, vol. 26, no. 6, pp. 990–994, 2008, in Chinese.

[17] W. Tian and P. Zhang, "Frozen-thaw damage test of concrete pore structure based on CT technology," *Journal of Central South University*, vol. 11, pp. 3069–3075, 2017, in Chinese.

[18] R. Chen and Y. Chen, "Study on mechanical properties after concrete freeze-thaw cycle," *Construction Safety*, vol. 04, pp. 70–73, 2018, in Chinese.

[19] S. Liang, "Study on the compressive strength of the concrete under the freeze-thaw cycle," *Science and Technology & Innovation*, vol. 13, pp. 139-140, 2019, in Chinese.

[20] V. N. Vapnik, *Estimation of Dependence Based on Empirical Data*, Springer-Verlag, Berlin, Germany, 1982.

[21] V. N. Vapnik, "An overview of statistical learning theory," *IEEE Transactions on Neural Networks*, vol. 10, no. 5, pp. 988–999, 1999.

[22] S. S. Keerthi and C. J. Lin, "Asymptotic behaviors of support vector machines with Gaussian kernel," *Neural Computation*, vol. 15, no. 7, pp. 1667–1689, 2003.

[23] National Standard of the People's Republic of China, *GB/T50082-2009 Standard For Test Methods of Long-Term Performance and Durability of Ordinary concrete*, China Architecture and Building Press, Beijing, China, 2009, in Chinese.

[24] X. Liu, *Research on SVM-Based Structural Damage Identification Method"*, Harbin Institute of Technology, Harbin, China, 2008, in Chinese.

[25] V. Cherkassky and Y. Ma, "Practical selection of SVM parameters and noise estimation for SVM regression," *Neural Networks*, vol. 17, no. 1, pp. 113–126, 2004.